Waveguiding power
of photonic crystal slabs

Serge Luryi and Arsen V. Subashiev*

Department of Electrical and Computer Engineering,
State University of New York at Stony Brook,
Stony Brook, NY, 11794-2350, USA
*Corresponding author: Subashiev@ece.sunysb.edu

Abstract

We consider the waveguiding by thin patterned slabs embedded in a homogeneous medium. In the longwave limit, the wave spectra of slabs are found to be well described by a single frequency-independent parameter, which we call the "guiding power". The guiding power can be evaluated in an effective medium approximation, similar to the Maxwell Garnett theory, but modified for the local field corrections specific to the two-dimensional geometry. The guiding power is different for the transverse magnetic (TM) and transverse electric (TE) polarizations. We show that the confinement factor of TM waves in a porous layer with high index ratio can exceed that for a homogeneous layer. Similarly enhanced confinement of TM waves is demonstrated for a layer of elongated cylinders or elliptic inclusion with a high axis length ratio. The effect originates from the suppression of local field effects and the increasing internal field in the inclusion. It may be useful in the design of far-infrared or THz quantum cascade lasers.

1 Introduction. Guiding power

Waveguiding of light in layered patterned structures, such as slabs of two-dimensionally periodic photonic crystals (2D PC), has attracted much in-

terest in view of potential photonic applications [1, 2, 3]. The studied 2D patterns include periodic lattices of deep etched air pores or "conjugate" lattices of high permittivity cylinders. The patterned slabs (not necessarily periodic) can be employed in waveguides as either a core or a cladding. Numerous theoretical computations of the band spectra of 2D PC and PC slabs have been reported, based on expansions of the electromagnetic field in plane waves [4, 3] or cylindrical waves [5, 6], as well as based on finite-difference time-domain methods [7, 8].

The low-frequency region of electromagnetic waves in the 2D PC is well understood. The waves have a linear spectrum that is very close to that obtained in the effective media approximation [9, 10] with an effective permittivity corresponding to the Maxwell Garnett theory [9, 11]. This means that when the wavelength λ exceeds the structure period a, the optical properties are primarily determined by the filling factor f of the inclusions (i.e. their total volume fraction) and do not rely on their long-range order or their shape variation. The disorder leads to a weak (for $\lambda \gg a$) Rayleigh-like scattering.

In this paper we investigate the waveguiding by PC slabs in a long wavelength frequency range, $qd \ll 1$, where q is the wave vector, d is the thickness of the active or a core layer of the waveguide. We show that in this range the waveguiding has a universal form described by a single parameter, which we call the "guiding power". For short-period structures, $d \gg a$, and for sparse structures, $d \ll a$, it can be calculated in terms of the polarizability of the patterned dielectric core via a self-consistent procedure to include local field effects.

We discuss the waveguiding in highly inhomogeneous structures, such as planar regular arrangements of nearly overlapping cylindrical pores or high-index cylindrical rods with large spacings. For thin slabs, the local field effects are different from those in an infinitely extended 2D PC, primarily because of the short-range dipolar interaction between the finite-height cylinders or spheres. Proper inclusion of the local field effects in the low-frequency region enables a perturbative approach with fast convergence.

In the design of far-infrared and terahertz semiconductor lasers the optical confinement is an important issue. It poses a severe problem for quantum cascade lasers where intersubband radiative transitions require transverse magnetic (TM) polarization of emitted waves [12]. With this polarization in the long wavelength region, the so-called modal confinement factor Γ_{TM} is known to be small for any contrast of the dielectric constants between the core and the claddings [13, 14]. The reason for the small values of Γ_{TM} is the reduced electric field in the high-index core due to the boundary conditions

at the core layer surface. The decrease of the electric field devalues traditional attempts to improve waveguiding by choosing cladding layers with lower index.

In this paper, we propose to enhance the confinement by using penetration of the electric field into a patterned core. The model core under consideration comprises additional cylinder inclusions of high dielectric constant compared to that of the claddings. The filling factor for these inclusions is small, so as not to disturb processes in the active region (which is the remainder of the core outside the inclusions). We show that the better penetration of the field can result in a much stronger waveguiding (much reduced field spread outside the layer), as compared to the homogeneous layer. This case has an advantage of not being critically sensitive to the composition of the claddings.

An alternative way to improve the guiding of TM waves is to use a porous PC slab as the active layer. We show that the confinement of TM modes in a structure with a high index contrast (typical for silicon-on-insulator devices) can be enlarged if the active layer has a patterned structure with pores. Even though the average index of the porous core is reduced, this is more than compensated by better penetration of the electric field into the structure, so that the wave confinement is ultimately enhanced.

Patterned structures with the enhanced confinement can be advantageously used in the laser design to minimize the losses from free-carrier absorption and reduce the threshold current.

An unusually strong guiding of TM waves in a layer of cylinders was previously observed in numerical studies of waveguiding by PC slab structures [15, 16] but the effect had not been properly recognized or explained.

2 Weakly guided waves in laterally uniform waveguides

In order to introduce the concept of weak waveguiding, let us first consider the propagation of an electromagnetic wave along a laterally uniform dielectric waveguide with a core layer. Let the index profile depend only on z, approaching at large $|z|$ the (background) dielectric constant ϵ_b of the cladding layers.

Two wave polarizations are distinguished by the field orientation relative to the structure symmetry plane. Consider the case of a TE mode, when the electric field has only an in-plane y component and is strictly perpendicular to the wave propagation direction x. The wave equation for the electric field

$E_y = E_y(z) \exp(iqx)$ is of the form

$$\frac{d^2}{dz^2} E_y(z) = [q^2 - k_0^2 \epsilon(z)] E_y \ , \tag{1}$$

where $\mathbf{q}$ is the 2D wave vector in the plane of the waveguide. Let us integrate Eq. (1) between $-z_1$ and z_1, that is over the region where the permittivity is variable. At $|z| \geq z_1$ the solution of the Eq. (1) has the form $E_y(z) = E(0) \exp(\pm \kappa z)$ and we get

$$-2\kappa E_y(0) = \int_{-z_1}^{z_1} [q^2 - k_0^2 \epsilon(z)] E_y(z) dz \ . \tag{2}$$

In the limit of weak waveguiding, $\kappa z_1 \ll 1$, the field $E_y(z)$ is a slowly varying function across the entire layer. Therefore it can be replaced in the integral by a constant value taken, e.g., at $z = 0$. Outside the guiding layer we have $q^2 = \epsilon_b k_0^2 + \kappa^2$ and hence in Eq. (2) we can take $q^2 = \epsilon_b k_0^2$ as the zeroth-order approximation. This yields

$$\kappa = \frac{1}{2} \epsilon_b k_0^2 \int_{-\infty}^{\infty} \left(\frac{\epsilon(z)}{\epsilon_b} - 1 \right) dz \ . \tag{3}$$

We have replaced the limits of integration by $\pm\infty$, since the region where $\epsilon(z) = \epsilon_b$ does not contribute to the integral in Eq. (3).

Similar arguments can be used to consider the waveguiding of TM waves, when the only non-vanishing component of the magnetic field is H_y. For this case, in the long wavelength limit, the quantity that remains a smoothly varying function across the layer is the normal component of the electric displacement vector D_z. Integrating the wave equation for D_z we obtain

$$\kappa = \frac{1}{2} \epsilon_b k_0^2 \int_{-\infty}^{\infty} \left(1 - \frac{\epsilon_b}{\epsilon(z)} \right) dz. \tag{4}$$

For both polarizations the dispersion relation for the guided wave is of the form

$$\epsilon_b k_0^2 = q^2 - \kappa^2, \tag{5}$$

where $k_0 = \omega/c$ is the frequency parameter. Parameter κ describing the exponential decay of the wave away from the core, $\exp(-\kappa z)$, depends on frequency. Since $\kappa \propto k_0^2$ the spectrum of the guided wave in the long-wavelength limit has a universal character. It is convenient to introduce another parameter g,

$$\kappa = \frac{1}{2} \epsilon_b k_0^2 g, \tag{6}$$

which we shall call the "guiding power" of the high-index core. The value of g defined by Eq. (6) is owing to the fact that it is frequency-independent in the weak guiding limit, $\kappa d \ll 1$ [13]. So long as g is constant, Eqs. (5, 6) define a universal dispersion relation for the guided modes of a three-layer dielectric waveguide of core thickness d.

According to Eqs. (3) and (4), the guiding power is given by :

$$g_{\mathrm{TE}} = \int_{-\infty}^{\infty} \left(\frac{\epsilon(z)}{\epsilon_b} - 1 \right) dz , \quad g_{\mathrm{TM}} = \int_{-\infty}^{\infty} \left(1 - \frac{\epsilon_b}{\epsilon(z)} \right) dz . \qquad (7)$$

For the simplest case of a constant permittivity (ϵ_g) core layer, Eqs. (7) reduce to

$$g_{\mathrm{TE}} = \frac{\epsilon_g - \epsilon_b}{\epsilon_b} d , \quad g_{\mathrm{TM}} = \frac{\epsilon_g - \epsilon_b}{\epsilon_g} d . \qquad (8)$$

In structures with a low index contrast, $(\epsilon_g - \epsilon_b) \ll \epsilon_b$, the values of g for both modes are small and close to each other. In the opposite limit, $(\epsilon_g/\epsilon_b) \gg 1$, the guiding power for the TM mode is ϵ_b/ϵ_g times weaker than g_{TE}, which can be explained by the reduced z component of the electric field inside the slab.

Confinement of guided waves is usually described by the dimensionless "confinement factor" Γ (fraction of the wave intensity that flows in the high-index core). Quite generally, Γ is proportional to the guiding power. The condition $\Gamma \ll 1$ corresponds to the *weak guiding limit*. In this limit the guiding power determines both the confinement properties and the dispersion of waves.

3 Waveguiding by a PC slab

Consider now the electromagnetic wave propagation along a photonic crystal slab formed either by a lattice of holes in a core layer or by a "mirror" structure with a set of cylinder rods serving as the core. In the long wavelength limit $\lambda \gg a, d$, where a is the PC lattice constant and d is the layer thickness, the field inhomogeneity is important only at short distances away from the slab, since the short-range components of the fields decay exponentially over the distances of order a. This allows us to identify the polarized waves as TE-like and TM-like. For $\lambda > d$ the weakly bound guided waves have a smooth exponential decay of the wave field away from the core, $E_z = E_{z,\,\mathrm{out}} \exp(-\kappa z)$ with $\kappa d \ll 1$. The relationship between κ and q can be obtained either by integrating the wave equation using the weak-guiding approximation (as in the preceding section) with averaging in the lateral

plane, or by using the effective media approach. The latter corresponds to replacing the PC layer by a homogeneous slab with an effective (anisotropic) dielectric constant [17]. Equations (5, 6) remain valid in both cases, but the guiding power g must now be evaluated taking account of the polarizability of the laterally inhomogeneous guiding layer.

Consider a core comprising a set of dielectric cylinders of radius r with the dielectric constant ϵ_{cyl} and height $d \gg r$. The cylinders are spaced apart with a lattice constant a and the core medium between the cylinders is assumed to have the same permittivity ϵ_b as the background. To compare the results with those of full-scale calculations, we further consider a square lattice of cylinders and the structure parameters close to those studied in [15, 16].

Importantly, the polarizability of a single cylinder is highly anisotropic. For a sufficiently elongated cylinder, $d/r \geq 5$, the polarization vector inside the cylinder is homogeneous and equal to that of an ellipsoid with a high axes length ratio. Besides, one must allow for depolarization effects. We take them into account approximately, by replacing the cylinders by prolate ellipsoids with the same diameter and the same volume, so that the axes length ratio of the ellipsoid $R_e = 3/4(d/r)$. The dipole moment of a single cylinder in an external electric field equals $P_z = V\alpha_z E_z$, where $V = \pi r^2 d$ is the cylinder volume and the polarizability of a single cylinder α_z is given by

$$\alpha_z = \frac{1}{4\pi}\epsilon_b \frac{\epsilon_{\text{cyl}} - \epsilon_b}{\epsilon_b + (\epsilon_{\text{cyl}} - \epsilon_b)n_z} \ . \tag{9}$$

Here n_z is the depolarization factor [20]. Even though in our case $n_z \ll 1$, the product $\epsilon_{\text{cyl}} \, n_z$ cannot be neglected. The average dielectric function of the layer equals

$$\epsilon_{l, \, \parallel} = \epsilon_b + f\epsilon_b \frac{\epsilon_{\text{cyl}} - \epsilon_b}{\epsilon_b + (\epsilon_{\text{cyl}} - \epsilon_b)n_z} \ . \tag{10}$$

The guiding power can now be calculated as in Eq. (8),

$$g_{\text{TM}} = d(1 - \epsilon_b/\epsilon_{l, \, \parallel}) \ , \tag{11}$$

and is given by

$$g_{\text{TM}, \ \text{cyl}} = d\frac{f(\epsilon_{\text{cyl}} - \epsilon_b)}{\epsilon_b + (f + n_z)(\epsilon_{\text{cyl}} - \epsilon_b)} \ . \tag{12}$$

The spectrum of the TE mode can be calculated in a similar way, with the transverse layer polarizability, $\epsilon_{l, \, \perp}$, expressed in terms of the transverse polarizability of a single cylinder, α_y. The result is similar to Eq. (9) except

194

for the depolarization factor, which should now be replaced by n_y. For a highly elongated cylinder, n_y is very close to 0.5, so that

$$\alpha_y = \frac{1}{2\pi} \epsilon_b \frac{\epsilon_{\text{cyl}} - \epsilon_b}{\epsilon_{\text{cyl}} + \epsilon_b} \ . \tag{13}$$

In calculating the average dielectric function $\epsilon_{l,\,\perp}$ of the layer one should take into account the local field effects (enhancement of the local field due to the field of surrounding cylinders). The simplest way to do this is to use the Maxwell Garnett approach, which is strictly applicable for $d \ll a$. In this approximation we have

$$\epsilon_{l,\,\perp} = \epsilon_b \frac{\epsilon_b + \epsilon_{\text{cyl}} + f(\epsilon_{\text{cyl}} - \epsilon_b)}{\epsilon_b + \epsilon_{\text{cyl}} - f(\epsilon_{\text{cyl}} - \epsilon_b)} \ . \tag{14}$$

The guiding power for TE waves is then given by

$$g_{\text{TE, cyl}} = 2d \frac{f(\epsilon_{\text{cyl}} - \epsilon_b)}{\epsilon_b + \epsilon_{\text{cyl}} - f(\epsilon_{\text{cyl}} - \epsilon_b)} \ . \tag{15}$$
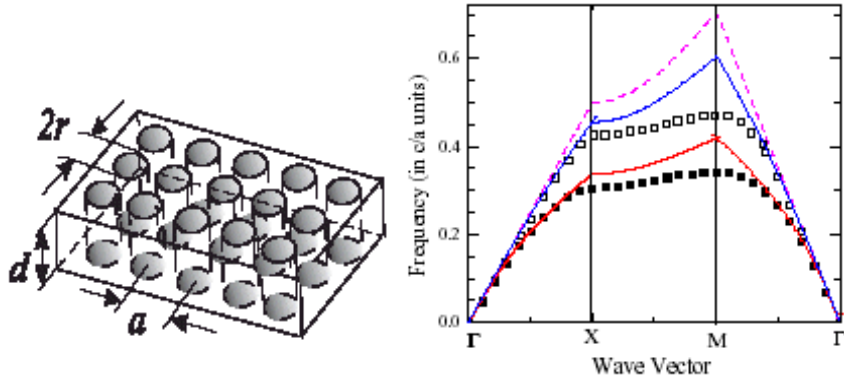

Figure 1: Low-frequency spectra of a photonic crystal slab composed of a square lattice of cylindrical rods (left panel) calculated in the "guiding power" approximation, Eqs. (5, 6). The TE mode is shown by a blue solid line, the TM mode by red line. Results of full-scale numerical calculations [15] are shown by open (TE) and closed (TM) dots. The dashed line indicates the light cone boundary. The filling factor is $f = 0.125$ and the cylinder's permittivity is $\epsilon_{\text{cyl}} = 12$.

The calculated spectra of TM and TE modes in the "guiding power" approximation are shown in Fig. 1 for a square lattice structure with $\epsilon_{\text{cyl}} = 12$, $\epsilon_g = \epsilon_b = 1$, $d/a = 2$, and $r/a = 0.2$ ($n_z = 0.03$). The results are compared with those of full-scale numerical calculations [15]. Our spectra shown in Fig. 1 do not include the effect of Bragg reflection, which can be allowed for by using a perturbative approach [19]. With Bragg reflections included [18], the guiding-power spectra approach the exact curves very closely.

Note that the guiding-power spectra are described by one parameter g for each mode. We can determine the values of these parameters by a best fit to the exact curves. In π/a units, the best-fit parameters are $g_{\text{TE}} = 1.2$ and $g_{\text{TM}} = 3.2$. These values can then be compared with those directly calculated from Eqs. (12,15), giving $g_{\text{TE, cyl}} = 1.5$ and $g_{\text{TM, cyl}} = 3.2$. For TE waves, the Maxwell Garnett approximation apparently overestimates the local field effects. If we use the polarizability of separate cylinders, we find $g_{\text{TE}} = 1.3$, which is closer to the best fit.

For the TM mode, which is of practical importance for intersubband lasers and is our main interest in this paper, the calculated value $g_{\text{TM, cyl}}$ provides an excellent approximation. We regard this very good agreement as a justification for applying the guiding power approach to calculations of the confinement factor. Note that due to the layer anisotropy, the waveguiding for TM waves is much stronger than that for TE waves.

Consider now the waveguiding in structures with a porous core layer. To calculate the guiding power for TM waves in this case, we use again Eq. (11). However, the depolarization effects are now very different. As is well known [20], these effects are important when the high-permittivity component has a convex shape, as is the case for cylinders. In contrast, for the cylindrical holes, the effect of depolarization can be essentially neglected, due to the concave shape of the high-permittivity component. Hence $\epsilon_{l,\,\|}$ is given by

$$\epsilon_{l,\,\|} = \epsilon_g + (\epsilon_b - \epsilon_g)f \ , \tag{16}$$

where the fraction of high-polarizability material in the core equals $1 - f$ for a film of porosity f. The resultant TM-wave guiding power is of the form

$$g_{\text{TM, por}} = d\frac{(1-f)(\epsilon_g - \epsilon_b)}{\epsilon_b + (1-f)(\epsilon_g - \epsilon_b)} \ . \tag{17}$$

196
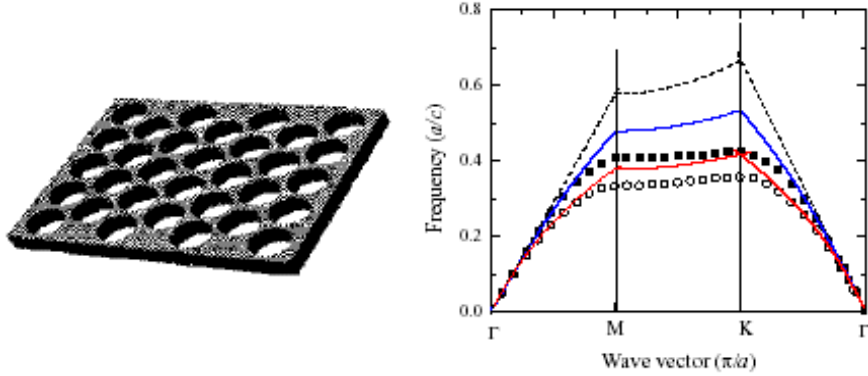
Figure 2: Low-frequency spectra of a photonic crystal slab formed by a dielectric layer with a triangular lattice of air holes with lattice constant a (left panel). Layer thickness is $d = 0.6a$, material permittivity is $\epsilon_g = 12$ and the hole radius is $r = 0.45a$. Results of the full-scale numerical calculation [15] are shown by open (for TM wave) and closed (TE) dots; red and blue lines show the spectra of TM and TE waves in the "guiding power" approximation; dashed line shows the edges of the light cone.

To calculate the guiding power for TE waves, we again use the Maxwell Garnett approximation, noting, however, that it is strictly applicable only for thick enough guiding layers, $d \gg r$ (this restriction is, of course, compatible with $\lambda \gg d$ required for the validity of the guiding power approximation). For a porous layer we find

$$\epsilon_{l,\,\perp} = \epsilon_g \frac{\epsilon_b + \epsilon_g + f(\epsilon_b - \epsilon_g)}{\epsilon_b + \epsilon_g - f(\epsilon_b - \epsilon_g)} \ , \tag{18}$$

whence the guiding power for TE waves is of the form

$$g_{\text{TE, por}} = d \frac{(1-f)(\epsilon_g^2 - \epsilon_b^2)}{\epsilon_b[\epsilon_b + \epsilon_g - f(\epsilon_b - \epsilon_g)]} \ . \tag{19}$$

To check these results against those of full-scale numerical calculations [15], we used Eqs. (5, 6) to calculate the TE and TM wave spectra for a triangular lattice of pores with $d = 0.6a$, and $r = 0.45a$ (the porosity $f = 0.734$), see Fig. 2. The values of g in π/a units that give best fit to the spectra are $g_{\text{TE}} = 3.1$ and $g_{\text{TM}} = 1.4$. The values calculated from Eqs. (17,19) are $g_{\text{TE, por}} = 3.4$ and $g_{\text{TM, por}} = 1.4$. As expected, the spectrum

197

of the TM guided wave is well described with an average dielectric constant of the core layer over most of the Brillouin zone up to the zone boundary, where it is strongly modified by the Bragg reflection. The Bragg reflection can be allowed using a perturbative approach [19, 18]. For a high-porosity layer of fairly small thickness, the spectrum of TE waves is also described by the guiding power approach, but the value of $g_{\text{TE, por}}$ is overestimated in the Maxwell Garnett approximation.

Note that both TM and TE waves remain weakly guided even in the extreme limit of sparse structures, $a \gg d$, so long as $\lambda \gg a$ [18].

4 Confinement factor of TM waves by a PC slab

The modal gain in a three-layer slab waveguide with an active core layer (ACL) of thickness d can be expressed as a product of the material gain, $G_{\text{ACL}} = k_0 n'' / \sqrt{\epsilon_{\text{ACL}}}$ and the dimensionless "optical confinement factor", Γ. For weakly guided TE waves with a smooth variation of the electric field of the wave across the layer, the confinement factor is just proportional to the guiding power, $\Gamma_{\text{TE}} = \kappa d = \epsilon_b k_0^2 d g_{\text{TE}}/2$. For TM waves the confinement is influenced by the weakening of the electric field in the high-permittivity core. Generally, it can be written in the form [14]

$$\Gamma_{\text{TM}} = \frac{\int_{\text{ACL}} E_z^2 dz}{\int_{-\infty}^{\infty} E_z^2 dz} \ , \tag{20}$$

where the integral in the numerator is taken over the active region. For a homogeneous core layer one can calculate the confinement factor explicitly. In the case of weak guiding, $\kappa d \ll 1$, using Eq. (20) and the boundary condition for the normal component of the field at the core edge planes, we find

$$\Gamma_{\text{TM}} = \frac{(k_0 d)^2}{2} \left(\frac{\epsilon_b}{\epsilon_g} \right)^3 \left(1 - \frac{\epsilon_b}{\epsilon_g} \right) \epsilon_g \ . \tag{21}$$

The value of Γ_{TM} is smaller than Γ_{TE} by a factor $(\epsilon_b/\epsilon_g)^3$. For a given core composition (i.e. for a fixed value of ϵ_g) and as a function of the cladding-layers index, Γ_{TM} has a maximum value,

$$\Gamma_{\text{TM, max}} \approx 0.05 \ \epsilon_g (k_0 d)^2 \ , \tag{22}$$

achieved when the ratio of the dielectric constants is $\epsilon_b/\epsilon_g = 3/4$. Note that $\Gamma_{\text{TM, max}}$ is about ten times smaller than the confinement of the TE mode achievable in the same structure. For a fixed value of ϵ_g, the factor Γ_{TE}

198

does not have a maximum, except at $\epsilon_b = 1$, where $\Gamma_{TE} \approx 0.5 \; \epsilon_g (k_0 d)^2 \approx 10 \; \Gamma_{TM, \; max}$. The difference in confinement factors is negligible in the structures with very small index contrast and thus very small confinement factors for both waves [17].

In the preceding section we showed that the TM waveguiding can be enhanced and even can exceed that for the TE mode by incorporating in the core layer cylindrical rods of high polarizability. We shall now show that the mode confinement in the *active part* of the core layer can be enhanced as well.

Consider the waveguiding in a patterned structure with initially small difference between the dielectric constant of the active layer (denoted by ϵ_g) and that of the cladding background, ϵ_b. Small values of $(\epsilon_g - \epsilon_b)$ are typical for quantum cascade lasers with a multilayer active region [12]. To enhance the waveguiding, we incorporate in the structure a set of cylindrical rods of radius r, lattice constant a, and dielectric constant ϵ_{cyl}. (Although we speak of the "lattice constant", the periodicity of rods is of no importance here and the result can be expressed in terms of their fill factor f.)
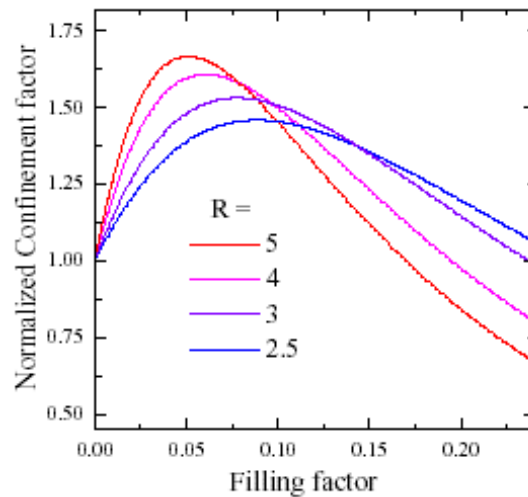

Figure 3: Normalized confinement factor for a PC slab with a square lattice of high-polarizability cylinders embedded in the core layer plotted as a function of f for several values of the ratio $R = \epsilon_{cyl}/\epsilon_g$, for $\epsilon_g = 12$ and $\epsilon_b = 11$.

For a waveguide with a patterned core layer, we first use the average dielectric constant to estimate the average field (which is somewhat different from the local field), and then use Eq. (20) to calculate the confinement factor of guided TM waves

$$\Gamma_{\text{TM}} = \frac{(k_0 d)^2}{2} \left(\frac{\epsilon_b}{\epsilon_{l, \parallel}} \right)^2 \left(1 - \frac{\epsilon_b}{\epsilon_{l, \parallel}} \right) (1 - f)\epsilon_g \ . \tag{23}$$

It can be seen from Eq. (23) that in structures with a high ratio $R = \epsilon_{\text{cyl}}/\epsilon_b$, the enhancement of waveguiding with f due to the increasing factor $(1 - \epsilon_b/\epsilon_{l, \parallel})$ can overwhelm at small f both the decrease in $(1 - f)$ and the decreasing factor $(\epsilon_b/\epsilon_{l, \parallel})^2$ that describes reduction of the electric field in the active layer.

The variation of the confinement factor, calculated with Eq. (10) [modified to include a term proportional to $(\epsilon_g - \epsilon_b)$] and Eq. (23), is plotted in Fig. 3. The increase of confinement with f is mainly due to the guiding power enhanced by the better polarizability of cylinders, hence it is most effective at small f. It can be seen from Eqs. (23) and (10) that the increase of confinement with f takes place only provided $\epsilon_g > 3(\epsilon_g - \epsilon_b) + 1$ and $\epsilon_{\text{cyl}} > 2\epsilon_g$. Note, that the increase of $\epsilon_{l, \parallel}$ with f towards the optimum value $\epsilon_{l, \parallel, \text{opt}}$ should be evaluated at fixed ϵ_b and ϵ_g (we have used $\epsilon_b = 11$ and $\epsilon_g = 12$). This gives $\epsilon_{l, \parallel, \text{opt}} = \sqrt(3)\epsilon_b$. For $\epsilon_{\text{cyl}} \gg \epsilon_g$ the optimum filling factor is small, $f \ll 1$, and the factor $1 - f$ is close to unity. In this most favorable case, the resulting confinement factor is larger than that for the initial homogeneous structure and approaches the optimal value given by Eq. (22).

The dependence of the confinement factor on the cylinder dielectric constant for $f = 0.05$ is shown in Fig. 4. In terms of the cylinder polarizability α_z (Eq. 9), the enhancement of confinement is well pronounced for $f\alpha_z > 20$, which can be achieved in the low-wavelength limit by inclusions of extremely highly-polarizable materials.

Next we consider the waveguiding in structures with a porous core layer. As seen from Eqs. (17), the guiding power of a porous active layer is smaller than that of a homogeneous layer for any ratio $R = \epsilon_g/\epsilon_b$ and is decreasing with f. However, for large R the decrease is small, while the rise of the electric field with the layer porosity provides an enhancement of the TM wave confinement.
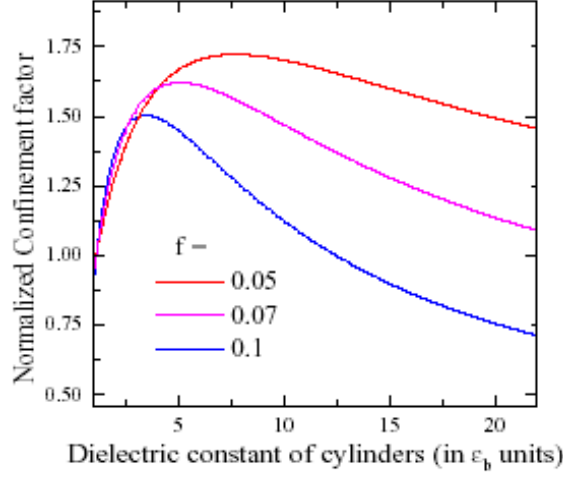
200

Figure 4: Normalized confinement factor as a function of ϵ_{cyl} for a PC slab with a square lattice of high-polarizability cylinders embedded in a core layer ($\epsilon_g = 12$) for several values of the filling factor. The background permittivity outside the core layer is $\epsilon_b = 11$.

Variations of the guiding power and the confinement factor with the porosity f for several values of the ratio R are shown in Fig. 5. For a given R, the maximum value of Γ_{TM} is achieved at

$$f_{\text{max}} = \frac{R-3}{R-1} \ . \tag{24}$$

Hence, replacing the homogeneous layer by a porous layer can increase the modal gain only using materials with $R > 3$. The maximum value of Γ_{TM} is

$$\Gamma_{\text{TM, max}} = \frac{4R^3}{27(R-1)^2}\Gamma_{\text{hom}} \ , \tag{25}$$

where Γ_{hom} is the confinement factor for a homogeneous core layer of the same R. As seen from Eq. (25), the increase of confinement by porosity can be tangible only for structures with large R. For Si/SiO$_2$ structures with $R = 6$ the maximal confinement enhancement is achieved at $f = 0.6$, but it is not very large (1.28); for $R = 12$ the enhancement is 2.1.
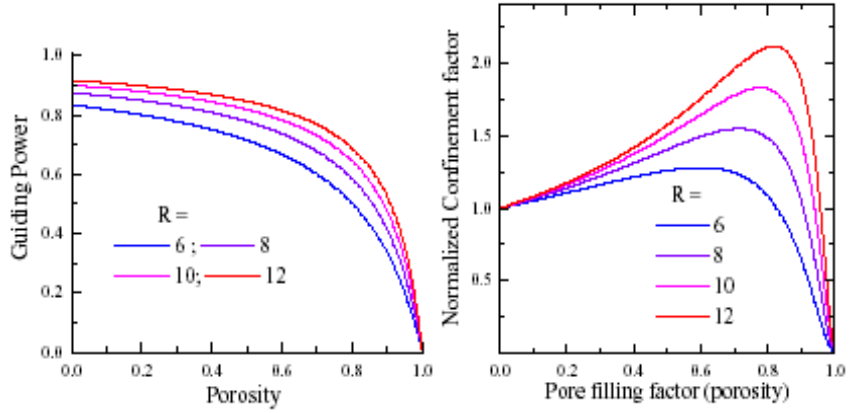
Figure 5: Porosity dependence of the guiding power g_{TM} (in units of d, left panel) and the normalized confinement factor Γ_{TM} (right panel) for a PC slab with a porous core layer. Both parameters are plotted as functions of the porosity f for several values of $R = \epsilon_g/\epsilon_b$.

We remark that although the numerical values above can be determined more accurately with more elaborate numerical calculations, the increase of confinement by patterning initially homogeneous layers is an exact result for waveguide structures with a high enough index contrast between the core and the claddings. The result is based solely on the power-law f dependencies of the guiding parameter g_{TM} and the field ratio inside the active layer.

5   Conclusions

In conclusion, we considered the polarization-dependent waveguiding of light by thin highly inhomogeneous slabs embedded in a uniform medium. We examined exemplary slab structures comprising a monolayer of patterned cylindrical pores etched in a active core layer or a pattern of high-index dielectric rods (cylinders), embedded in the core layer. We demonstrated that for an optimal choice of the patterned layer structure an increase of optical confinement of TM wave is possible compared to a homogeneous layer. This increase can be achieved both by incorporating sparsely separated high-index rods which promote electric field penetration in the patterned structure and by using high-porosity core layers. Our results can be useful in the design

202

of quantum cascade lasers.

References

[1] E. Yablonovitch, T.J. Gmitter and K.M. Leung, Phys. Rev. Lett. **67**, 2295 (1991).

[2] O. Painter, R.K. Lee, A. Scherer, A. Yariv, J.D. O'Brien, P.D. Dapkus, and I. Kim, Science, **284**, 1819 (1999).

[3] J.D. Joannopoulos, R.D. Meade and J.N. Winn, *Photonic Crystals: Molding the Flow of Light*, (Princeton University, Princeton, NJ, 1995).

[4] M. Plihal and A.A. Maradudin, Phys. Rev. B **44**, 8565 (1991); V. Kuzmyak, A.A. Maradudin and A.R. McGurn, *ibid.* **55**, 4298 (1997).

[5] N.A. Nicorovici, R.C. McPhedran and L.C. Botten, Phys. Rev. E **52**, 1135 (1995).

[6] K. Ohtaka, T. Ueta and K. Amemiya, Phys. Rev. B **57**, 2550 (1998).

[7] A. Taflove, *Computational Electrodynamics – The Finite-Difference Time-Domain Method* (Artech House, Boston, MA, 1995).

[8] M. Boroditsky, R. Coccioli and E. Yablonovitch, *Analysis of photonic crystals for light emitting diodes using the finite difference time domain technique* (Photonics West, 1998).

[9] A.K. Sarychev and V.M. Shalaev, Phys. Rep. **335**, 275 (2000).

[10] A.A. Krokhin, P. Halevi and J. Arriaga, Phys. Rev. B **65**, 115208 (2002).

[11] N.A. Nicorovici, R.C. McPhedran, and L.C. Botten, Phys. Rev. Lett. **75**, 1507, 1995.

[12] O. Malis, C. Gmachl, D.L. Sivco, L.N. Pfeiffer, A.M. Sergent, and K.W. West, Bell Labs Tech. Journ. **10**, 199 (2005).

[13] D. Marcuse, *Theory of Dielectric Optical Waveguides* (Academic Press, Boston, 1991).

[14] T.D. Visser, H. Blok, B. Demeulenaere, and D. Lenstra, IEEE J. Quant. Electron. **33**, 1763 (1997).

[15] S. Johnson, S. Fan, P.R. Villeneuve, J.D. Joannopoulos, and L.A. Kolodziejski, Phys. Rev. B **60**, 5751 (1999).

[16] S. Johnson, P.R. Villeneuve, S. Fan, and J.D. Joannopoulos, Phys. Rev. B **62**, 8212 (2000).

[17] A.V. Subashiev and S. Luryi, IEEE J. Lightwave Techn. **24**, 1513 (2006).

[18] S. Luryi and A.V. Subashiev, Proc. of SPIE **6127**, 612705 (2006); online at http://www.ee.sunysb.edu/ serge/212.pdf.

[19] T. Ochiai and K. Sakoda, Phys. Rev. B **64**, 045108 (2001).

[20] L.D. Landau and E.M. Lifshitz, *Electrodynamics of Continuous Media* (Pergamon Press, Oxford, 1960).